4. Basins due to orogenic loading

Orogenic loading and lithospheric flexure: peripheral vs. retroarc foreland basin

Elastic vs. viscoelastic models

Gravity anomalies, foreland flexure, and the development of the mountain belts

Stratigraphic architecture of the foreland basins

Lithospheric strength and structural styles (thin- or thick-skinned deformation)
in the fold-and-thrust belt

Prepared by Dr. Andrew T. Lin
Institute of Geophysics
National Central Univ. Taiwan

Orogenic loading and lithospheric flexure: peripheral vs. retroarc foreland basin

Peripheral foreland basin

Retroarc foreland basin

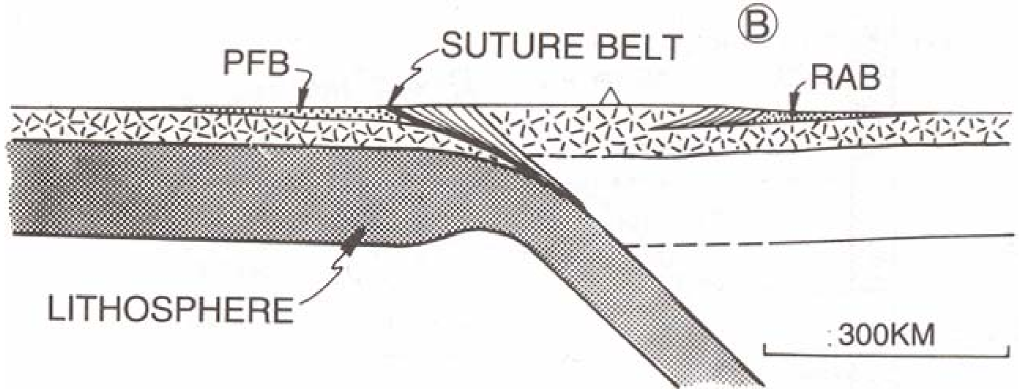

Foreland basins develop on continental crust in front of advancing thrust-and-fold loads along the length of subductional or collisional plate margins.

Roles of orogenic belts:

1. Load the underlying lithosphere
2. Provide sediments to the foreland basin

Two types of foreland basins

A. **Peripheral** foreland basins: lie on the continental crust of the subducting plate.
Examples: Active:Taiwan, Indo-Gangetic (Hymalayan frontal thrusts), Tigris-Euphrates-Arabian Gulf basins (Zagros Mountains)
Inactive: Molasse basins of the Alps and Pyrenees.

B. **Retroarc** foreland basin: (large scale and long life) lie on the continental crust of the overriding plate.

Examples:
1. Eastern foreland of the Rocky Mountains (Mesozoic to early Cenozoic)
2. Eastern foreland of the Andes (Jurassic to Recent)

Example of peripheral foreland basin: Taiwan

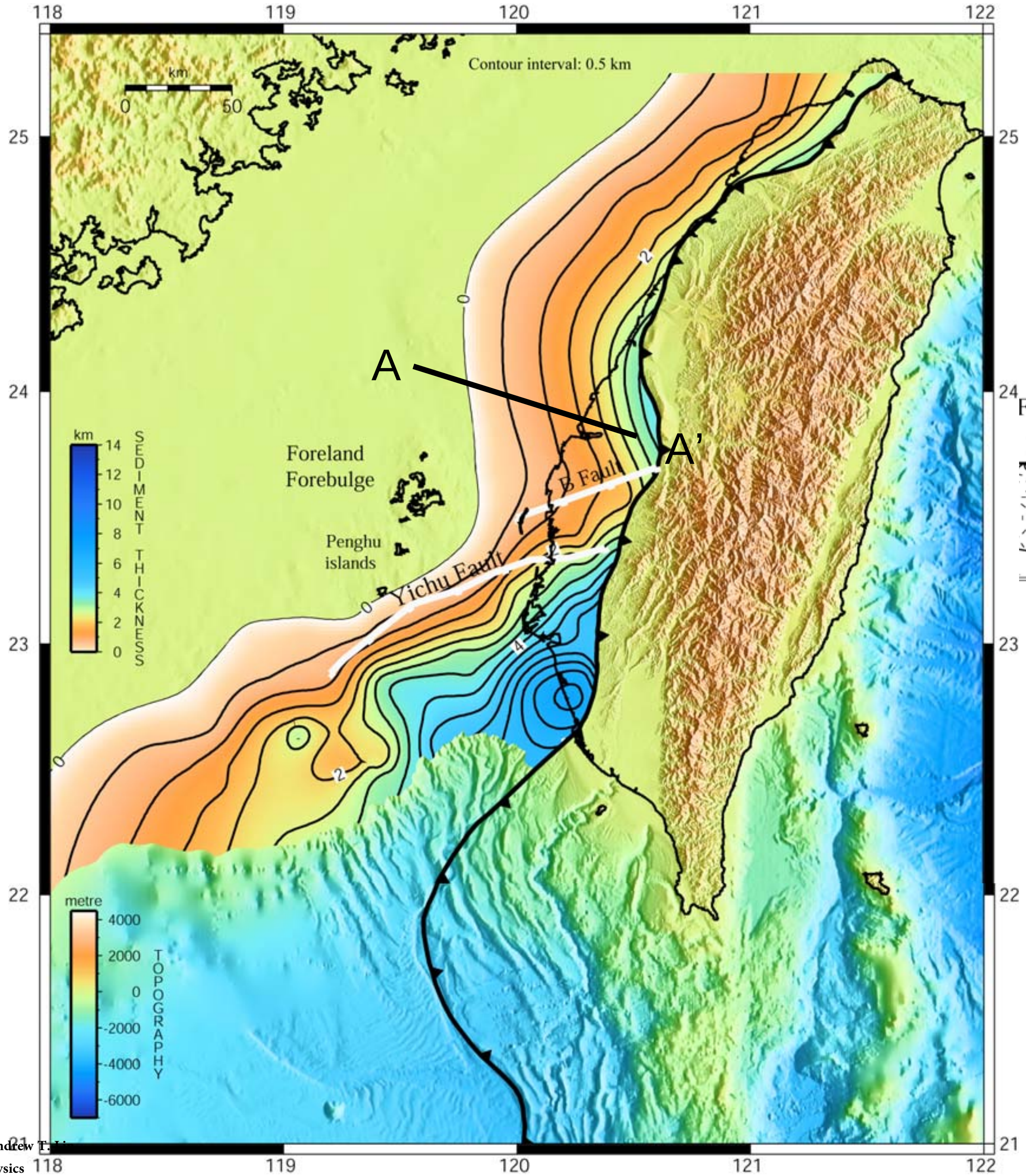

Depth map of the Taiwan foreland basin (Lin & Watts, 2002)

Contour interval 0.5 km

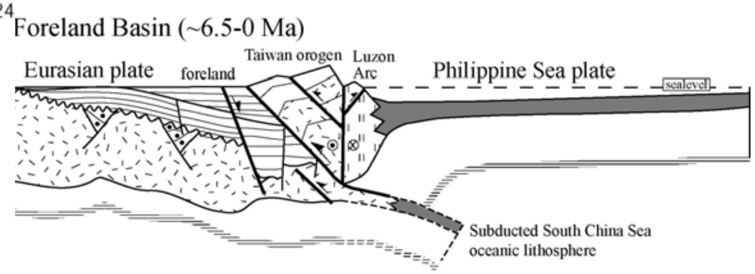

Lin et al. (2003)

Prepared by Dr. Andrew T. Lin
Institute of Geophysics
National Central Univ. Taiwan

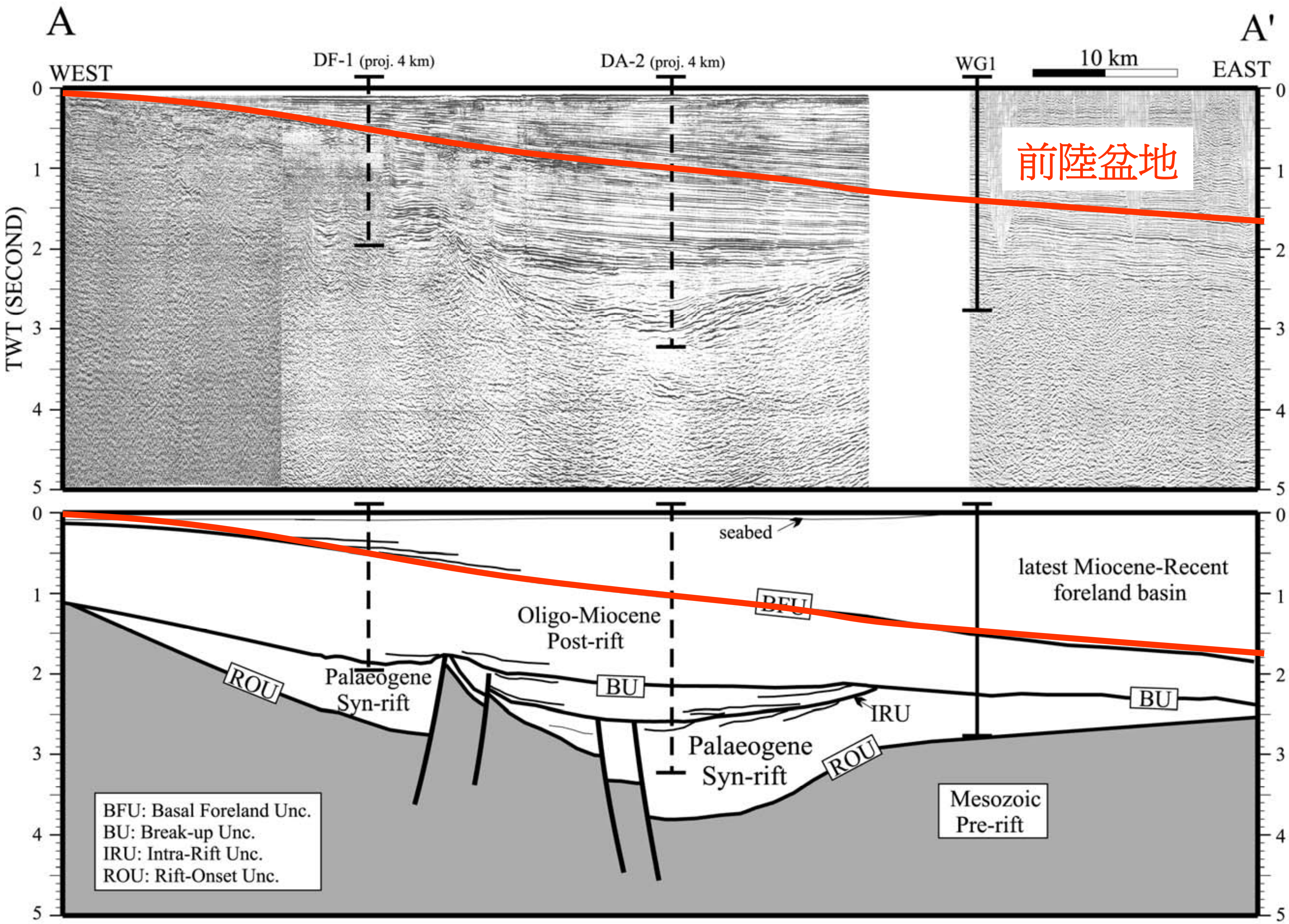

Lin & Watts (2002)

Appalachian foreland basin

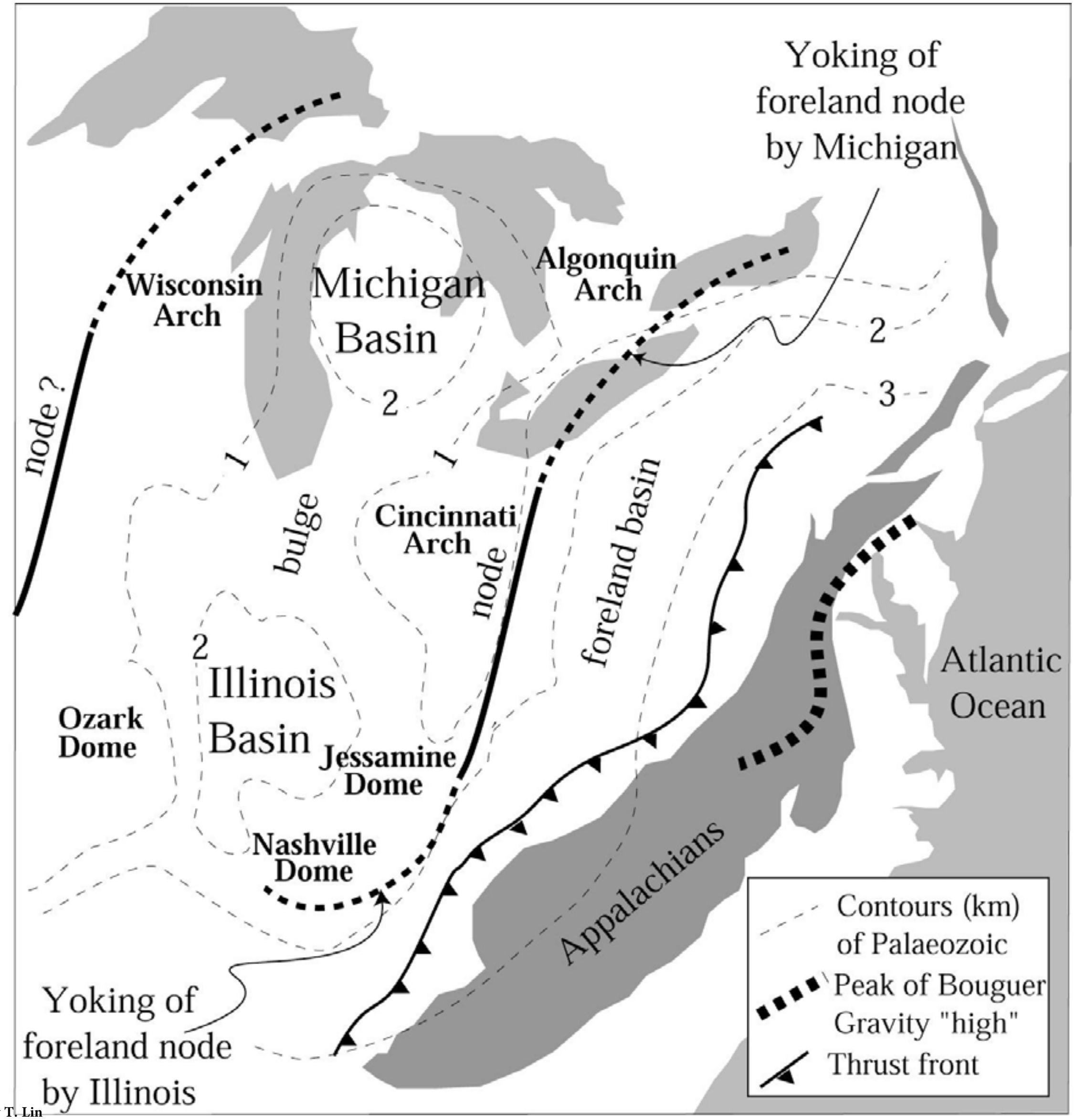

Watts (2001) redrawn from Karner & Watts (1983)

Flexural interactions between the Appalachian foreland basin and the Michigan and Illinois intra-cratonic basins could explain the existence of the arches and domes in the eastern US.

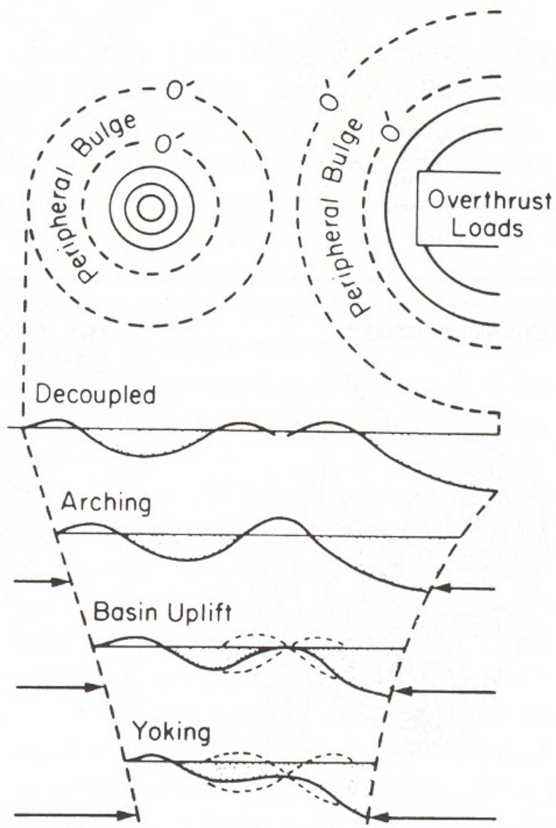

Quinlan & Beaumont (1984)

Prepared by Dr. Andrew T. Lin
Institute of Geophysics
National Central Univ. Taiwan

Example of retroarc foreland basins (Andes)

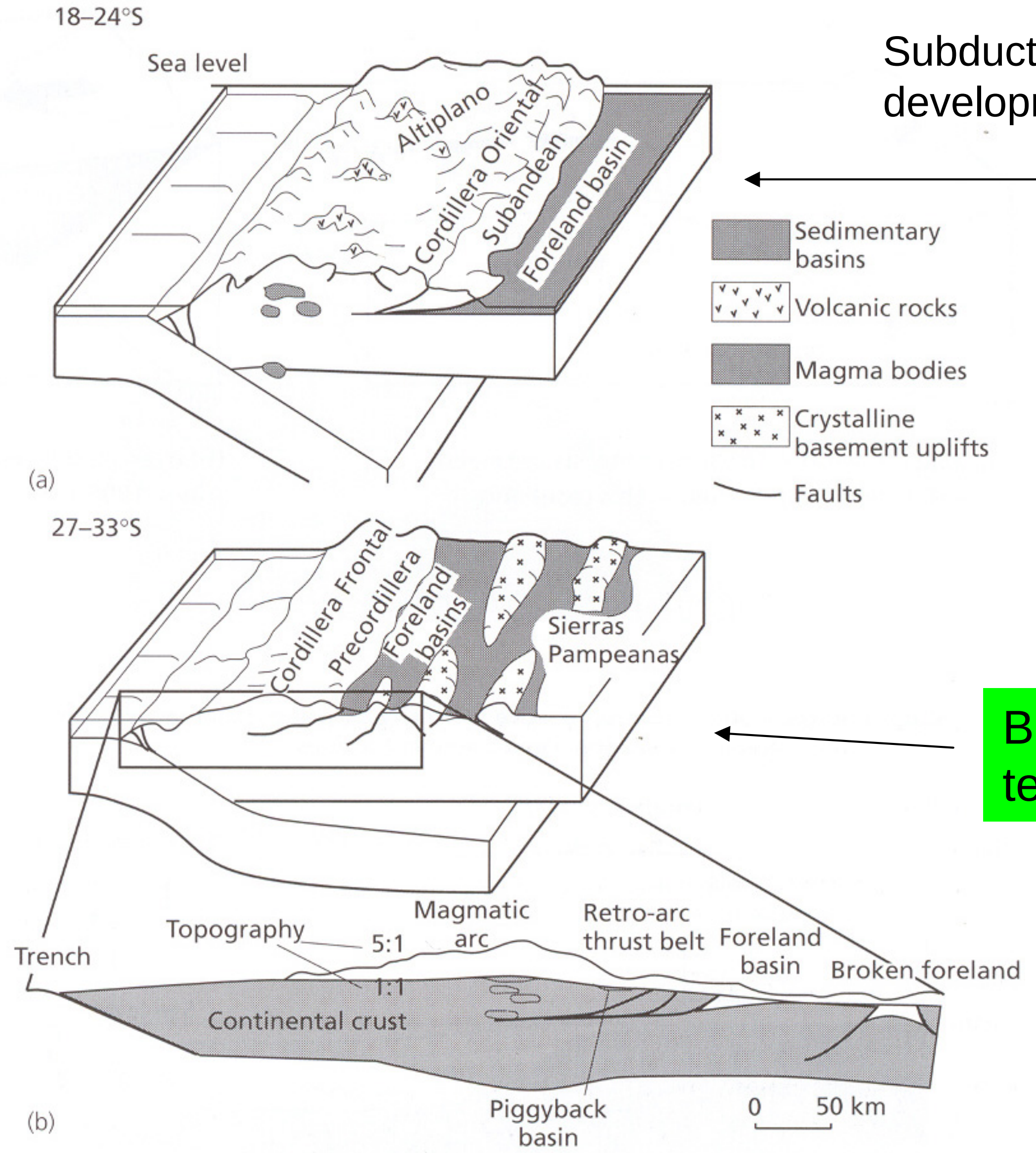

Subduction geometry and foreland basin development.

Thin-skin tectonics

Basement-involved (thick-skin) tectonics

Jordan (1995)

Appalachian foreland basins

The geometry of the foreland basin provides some of the best evidence on the thermal and mechanical properties of the continental lithosphere.

In a cross section that is perpendicular to the strike of the foreland basin,
the depths of the foreland base exponentially increase toward the orogen.

How the outermost layers of the Earth respond to loads of different duration

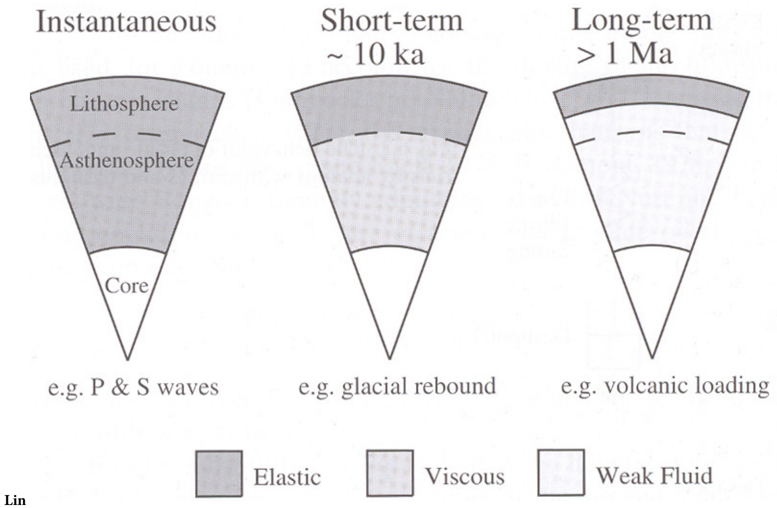

Watts (2001)

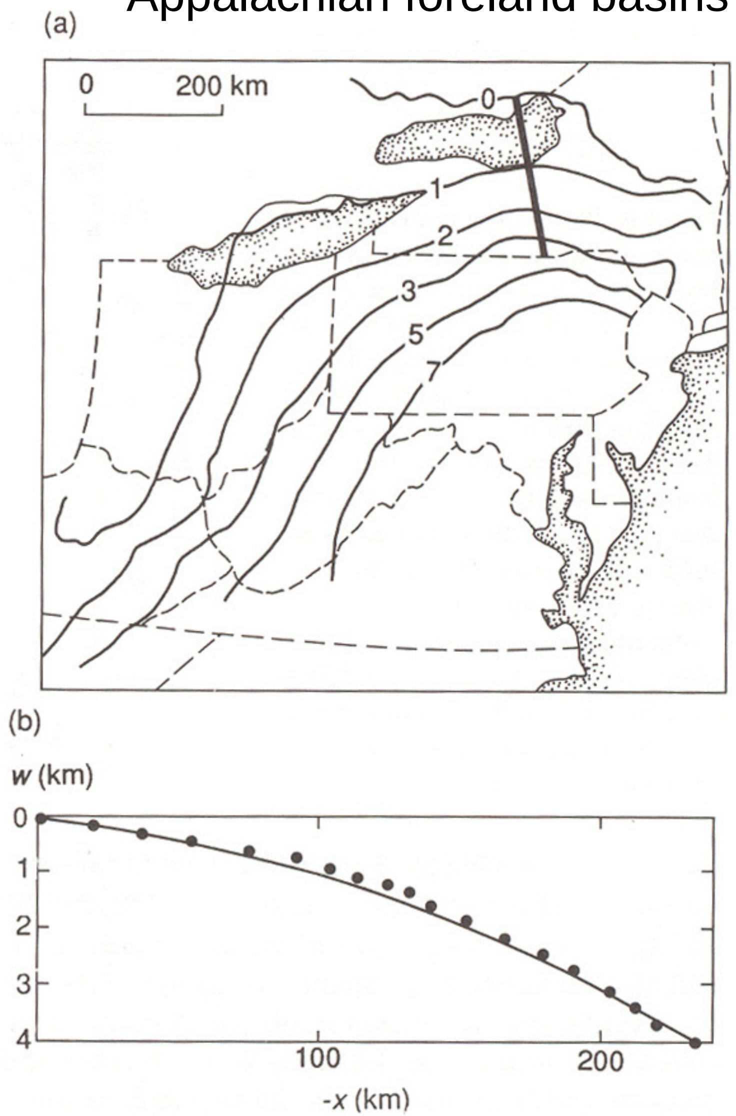

Turcotte & Schubert (1982) in Allen & Allen (1990)

Prepared by Dr. Andrew T. Lin
Institute of Geophysics
National Central Univ. Taiwan

Elastic Plate Theory

The comparison of observations (e.g. crustal structure) to calculations show that the response of the lithosphere to long-term loads is similar to what would be expected for an **elastic plate** that overlies an **inviscid** (i.e. zero viscosity) **substratum**.

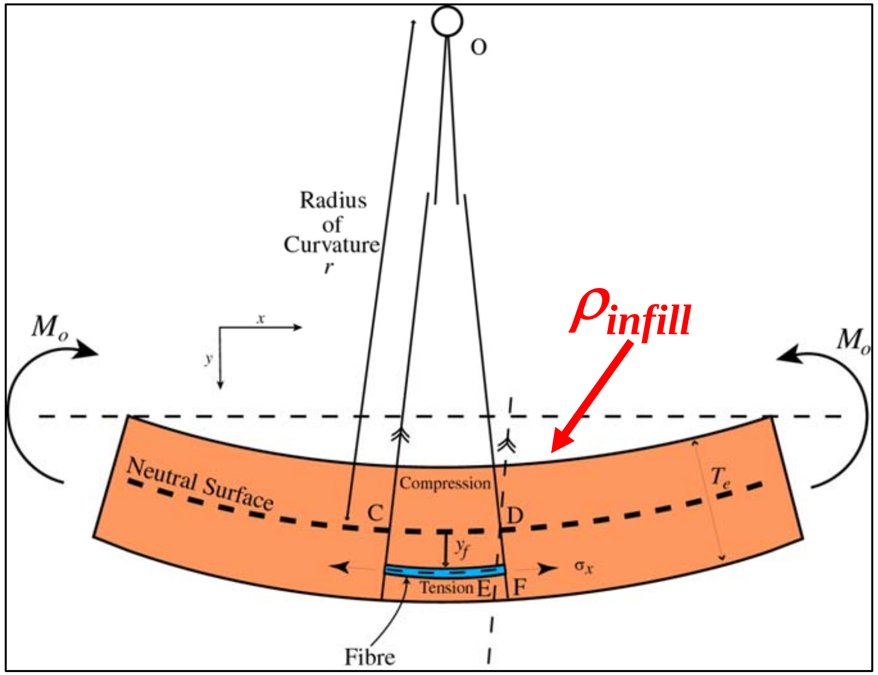

Equations:

The general equation for the flexure of an elastic plate overlying an inviscid substratum by an applied load can be derived by first determining the response of an elastic beam of unit width subject to an external bending moment, M_0.

$$D \frac{d^4 y}{dx^4} + (\rho_m - \rho_{infill})\, y\, g = 0$$

$$D = \frac{E\, T_e^3}{12\,(1-\nu^2)}$$

Parameters:

D = flexural rigidity
y = flexure
ρ_m = density of substratum
ρ_{infill} = density of material infilling flexure
E = Young's modulus
T_e = elastic thickness, ν = Poissons ratio

Assumptions:

1. Linear elasticity
2. Plane stress
3. Cylindrical bending
4. Thin plates (i.e. plate thickness << radius curvature)
5. Neutral surface, fixed at the half depth

Prepared by Dr. Andrew T. Lin
Institute of Geophysics
National Central Univ. Taiwan

Courtesy of Prof. A. B. Watts

The general equation for the deflection of an elastic beam can be solved for certain boundary conditions. Two of the most useful in geological applications are those for a continuous plate ($x \rightarrow \pm\infty$, $z \rightarrow 0$; $x = 0$, $dy/dx = 0$) and for a broken plate (e.g. end-conditioning forces).

Continuous plate :

$$y = \frac{P_b \lambda}{2\,(\rho_m - \rho_{infill})\,g} e^{-\lambda x}(\mathrm{Cos}\lambda x + \mathrm{Sin}\lambda x)$$

$$\lambda = \left[\frac{(\rho_m - \rho_{infill})\,g}{4\,D}\right]^{1/4}$$

$1/\lambda$ = flexural parameter

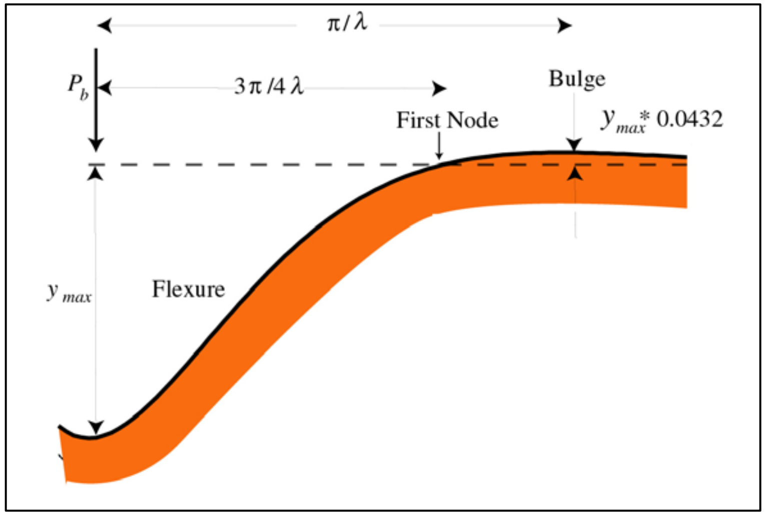

Broken plate :

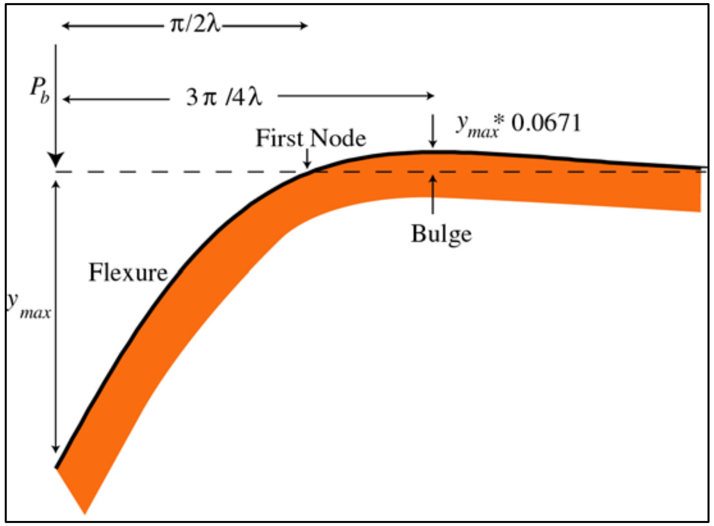

$$y = \frac{2\,P_b\,\lambda}{(\rho_m - \rho_{infill})\,g} e^{-\lambda x}\,\mathrm{Cos}\lambda x$$

Prepared by Dr. Andrew T. Lin
Institute of Geophysics
National Central Univ. Taiwan

Courtesy of Prof. A. B. Watts

Elastic vs. viscoelastic plates

(a) Elastic model $\sigma = E\varepsilon_e$

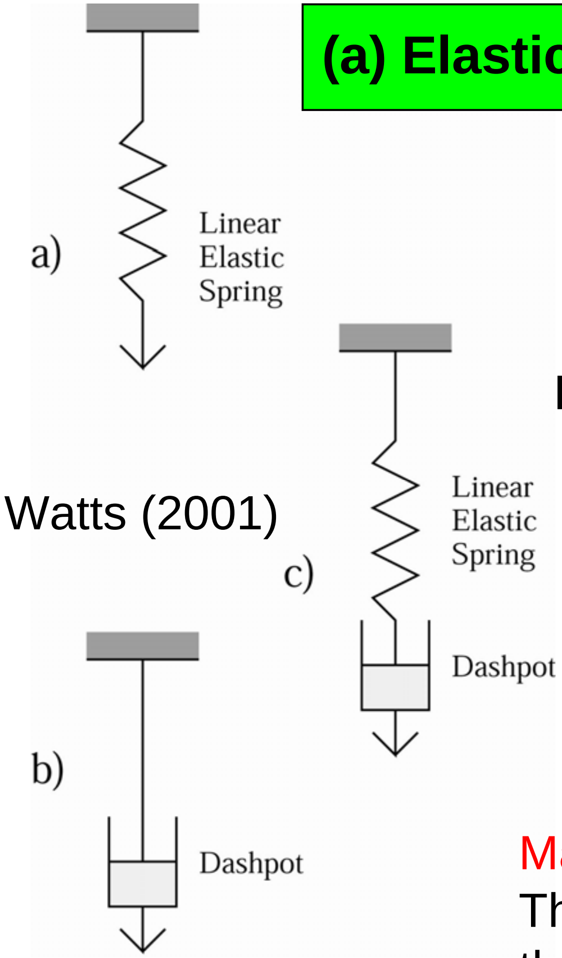

Watts (2001)

(C) Maxwell viscoelastic model (a+b)

Total strain: $\varepsilon = \varepsilon_e + \varepsilon_v$

If the system is initially unstrained – that is, ε=0 at t=0 –then

$$\varepsilon_e = \frac{\sigma}{E} \quad \text{and} \quad \dot{\varepsilon}_v = \frac{d\varepsilon_v}{dt} = \frac{\varepsilon_v(t) - \varepsilon_v(0)}{t - t_0} = \frac{\varepsilon_v}{t} \longrightarrow \varepsilon_v = \frac{t\sigma}{\eta}$$

$$\therefore \varepsilon = \frac{\sigma}{E} + \frac{\sigma \cdot t}{\eta}$$

The viscoelastic strain is made up of both and elastic and a viscous part.

(b) Viscous model

$\sigma = \eta\dot{\varepsilon}_v$

Maxwell relaxation time (τ):
The time when the elastic strain that has accumulated is equal to that of the viscous train.

$$\tau = \frac{\eta}{E}$$

~ 0.1 to severalc Myr or 1 to 100 Myr (Watts, 2001, p.244)

Parameters:
- E = Young's modulus
- η = viscosity
- ε_e = elastic strain
- $\dot{\varepsilon}_v$ = viscous strain rate
- σ = stress
- τ = Maxwell relaxation time

Prepared by Dr. Andrew T. Lin
Institute of Geophysics
National Central Univ. Taiwan

A viscoelastic plate is initially elastic and then becomes more viscous as the age of the load increases.

Deflection of a viscoelastic plate by
(a) a “wide” and
(b) a “narrow” load.

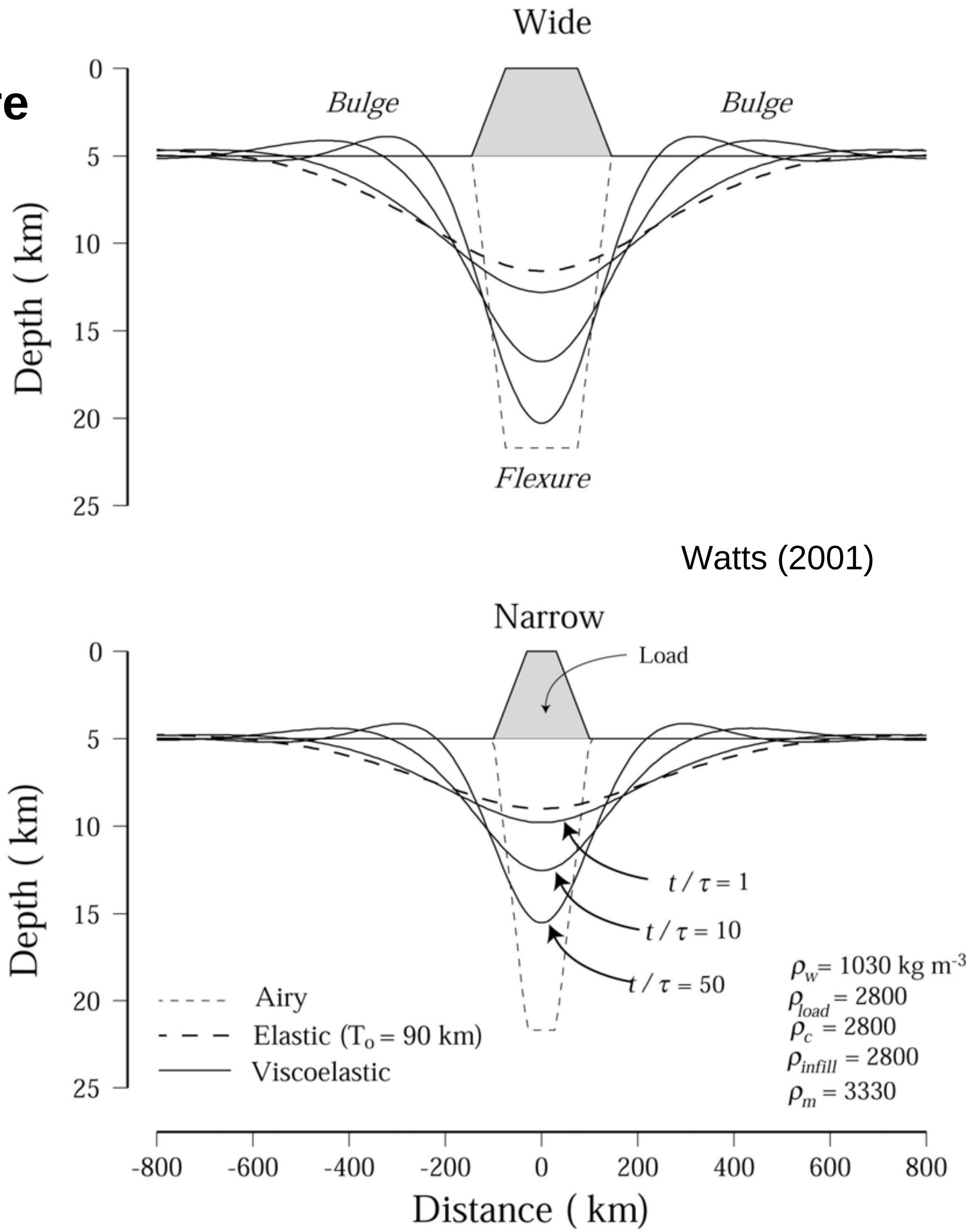

Watts (2001)

Prepared by Dr. Andrew T. Lin
Institute of Geophysics
National Central Univ. Taiwan

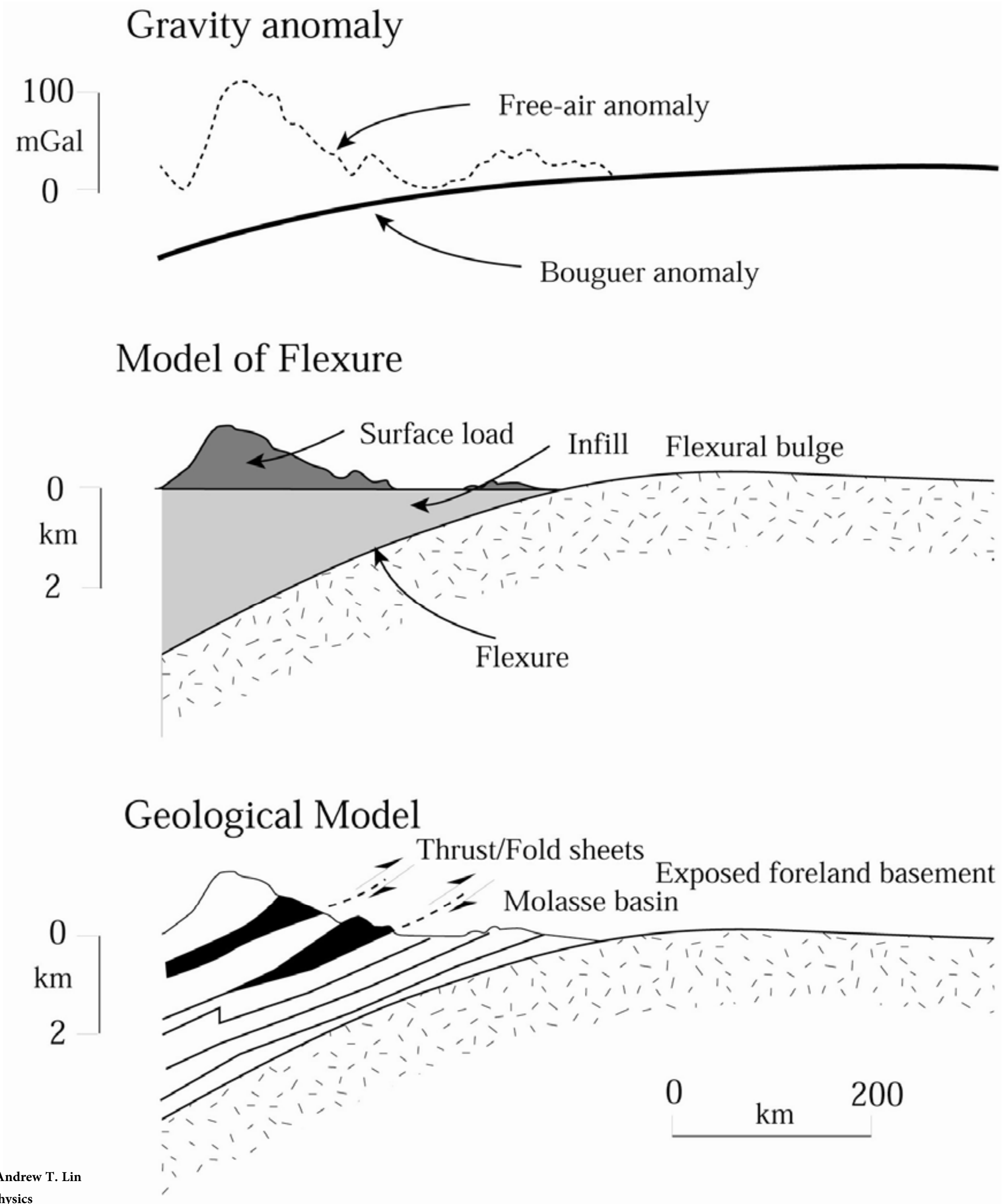

Watts (2001) redrawn from Karner & Watts (1983)

Gravity anomalies and flexure of the lithosphere caused by surface loading at the edge of an orogenic belt.

Prepared by Dr. Andrew T. Lin
Institute of Geophysics
National Central Univ. Taiwan

The interiors of large orogenic belts are generally in a state of isostatic equilibrium (i.e., Airy isostasy), their edges show large departures (i.e., flexure).

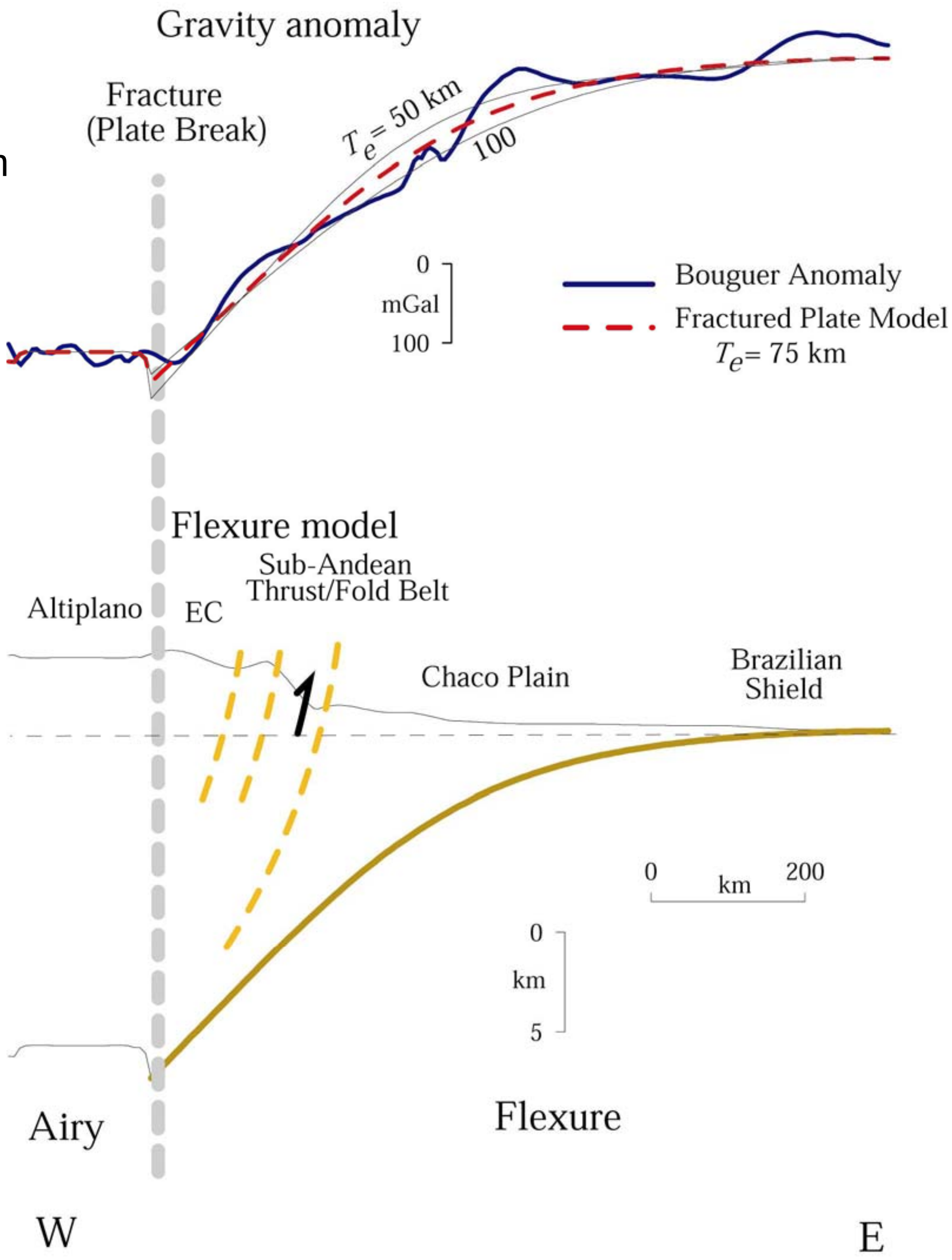

Paper:
Lin, A. T. & Watts, A. B. (2002) Origin of the West Taiwan Basin by orogenic loading and flexure of a rifted continental margin.
Journal of Geophysical Research, 107(B9), 2185, doi:10.1029/2001JB000669.

Prepared by Dr. Andrew T. Lin
Institute of Geophysics
National Central Univ. Taiwan

Stratigraphic architecture of the foreland basins

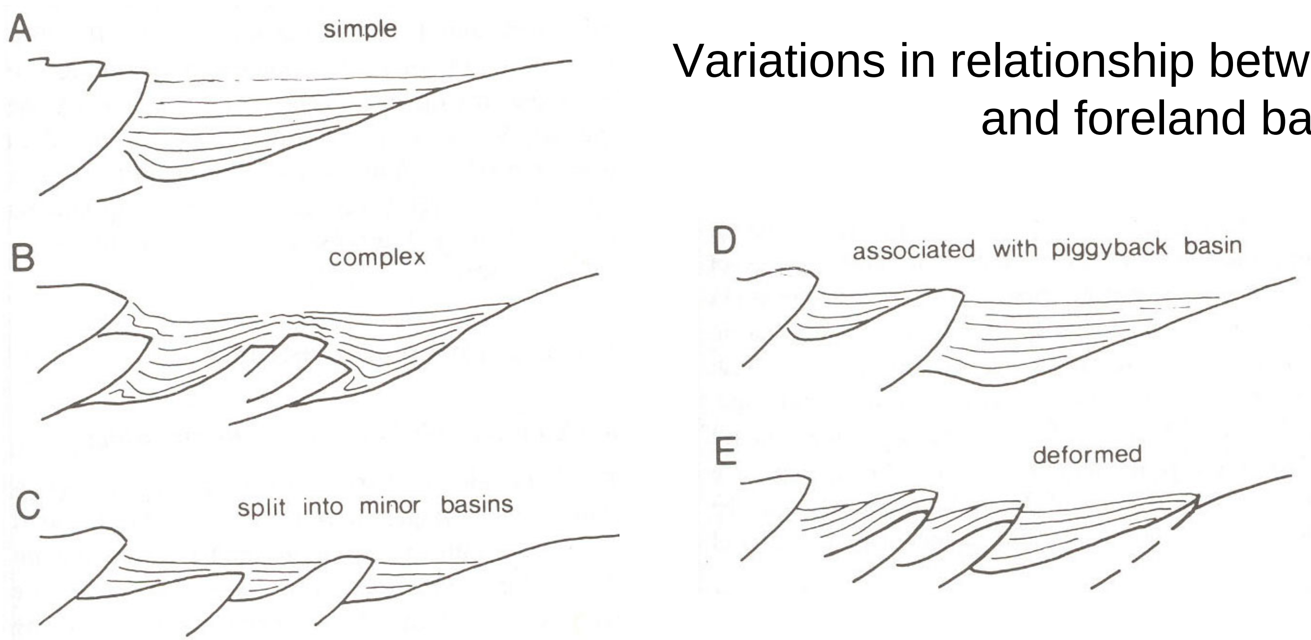

Variations in relationship between fold-thrust belt and foreland basins.

Ricci-Lucchi (1986)

Depo-zones in an idealized foreland basin system (Horton & DeCelles, 1997)

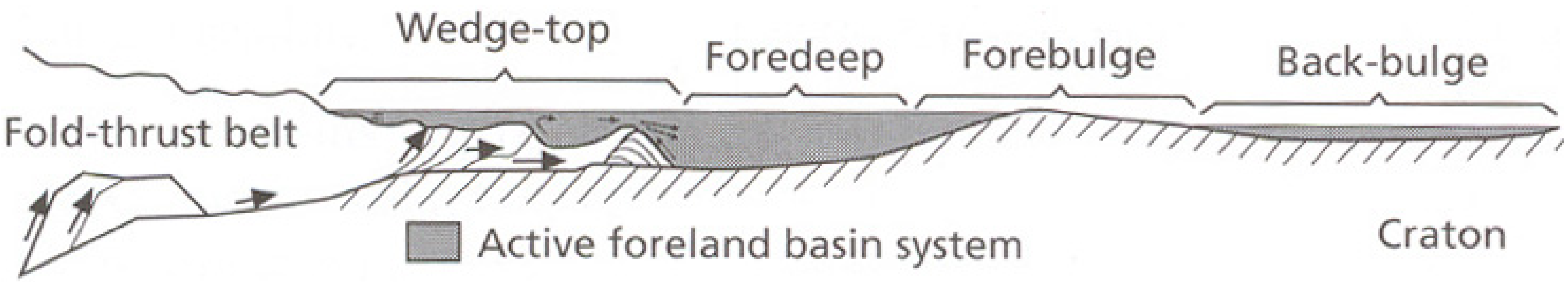

Note: The origin of the back-bulge is poorly known.

Prepared by Dr. Andrew T. Lin
Institute of Geophysics
National Central Univ. Taiwan

An example of a piggyback basin

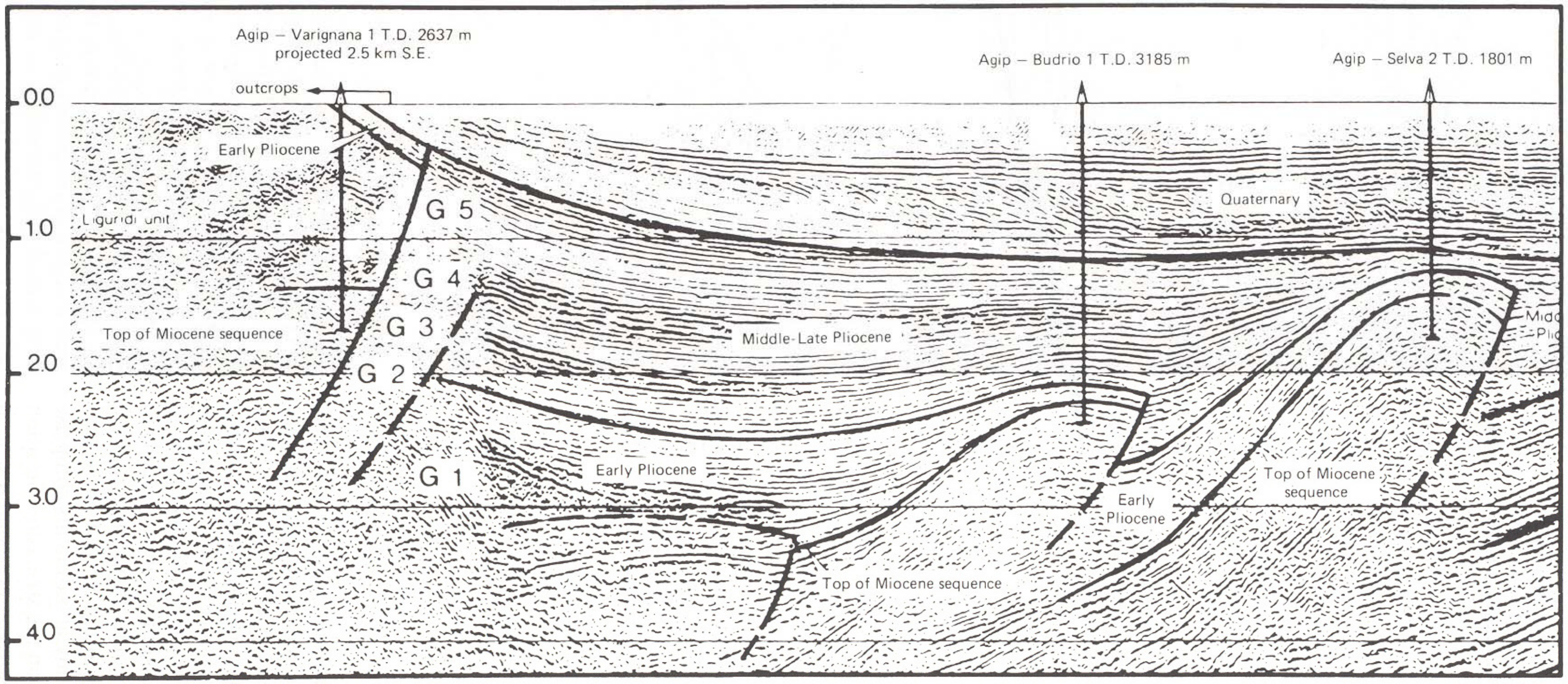

Fig. 9.69. Example of a seismic transect across the edge of a foreland basin, showing blind thrusts and sediment drape over them. The main basin, filled with Pliocene sediment at the *center*, is an example of a satellite, or piggyback, basin. (Ricci-Lucchi 1986)

Prepared by Dr. Andrew T. Lin
Institute of Geophysics
National Central Univ. Taiwan

Development of a fold-thrust belt and the stratigraphy of the adjacent foreland basins (piggyback basins)

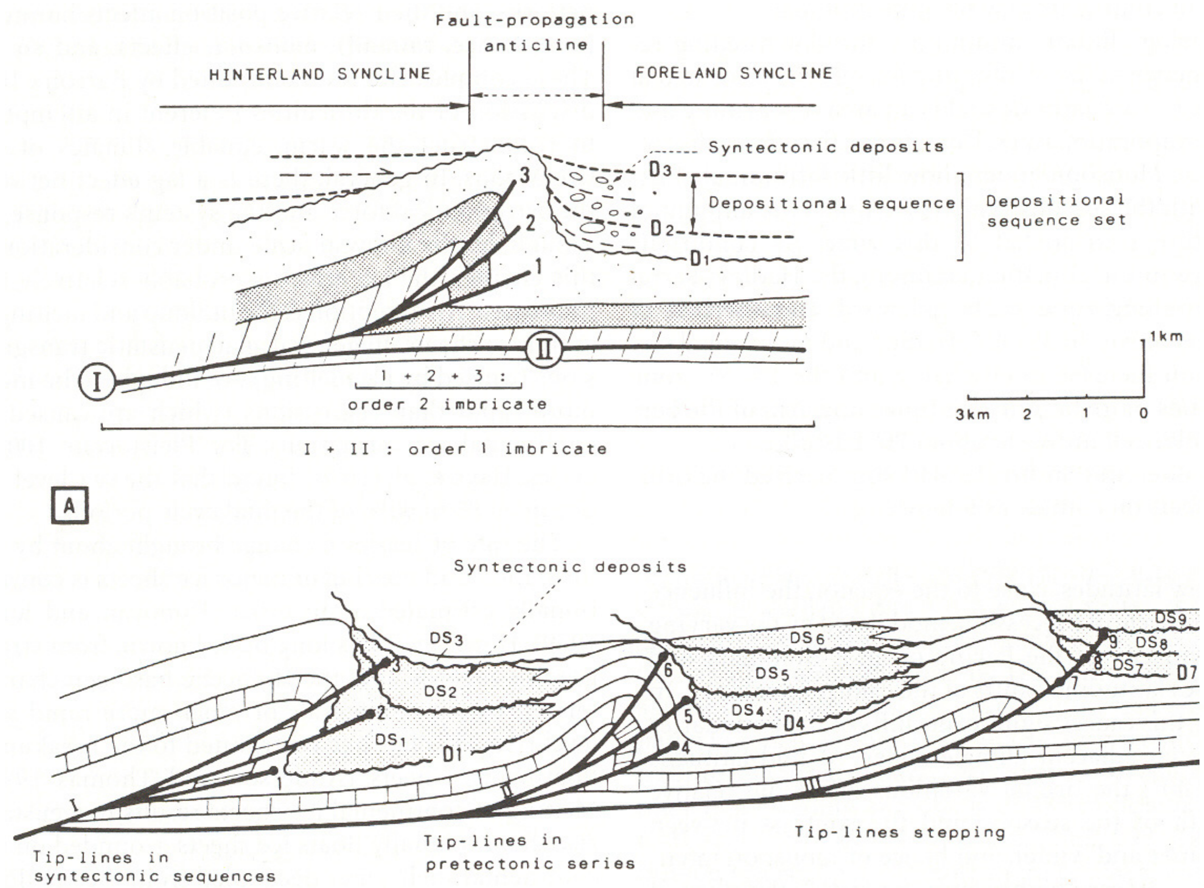

Deramond et al. (1993)

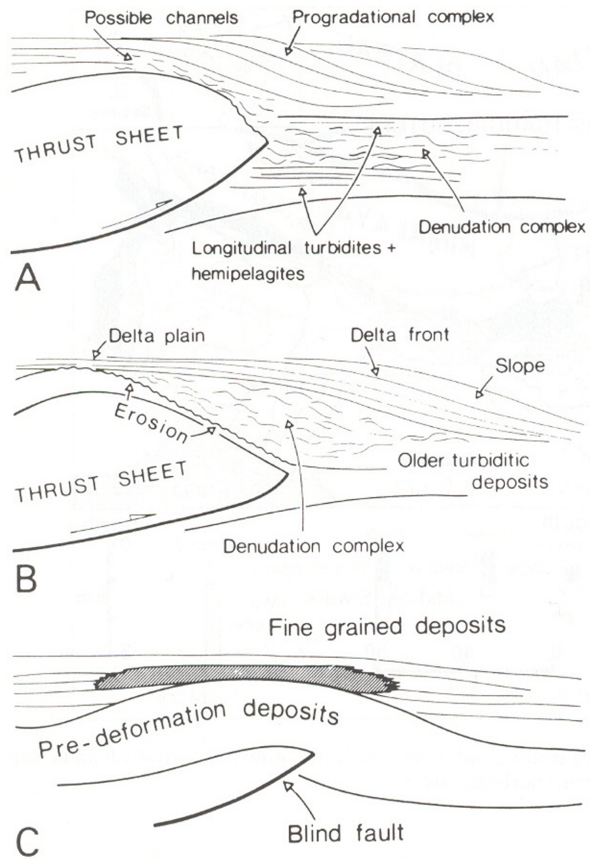

Ori et al. (1986)

Unconformities (D1~D9) develop as imbricate thrust slices develop.

Prepared by Dr. Andrew T. Lin
Institute of Geophysics
National Central Univ. Taiwan

Stratigraphy of the North Alpine foreland basin

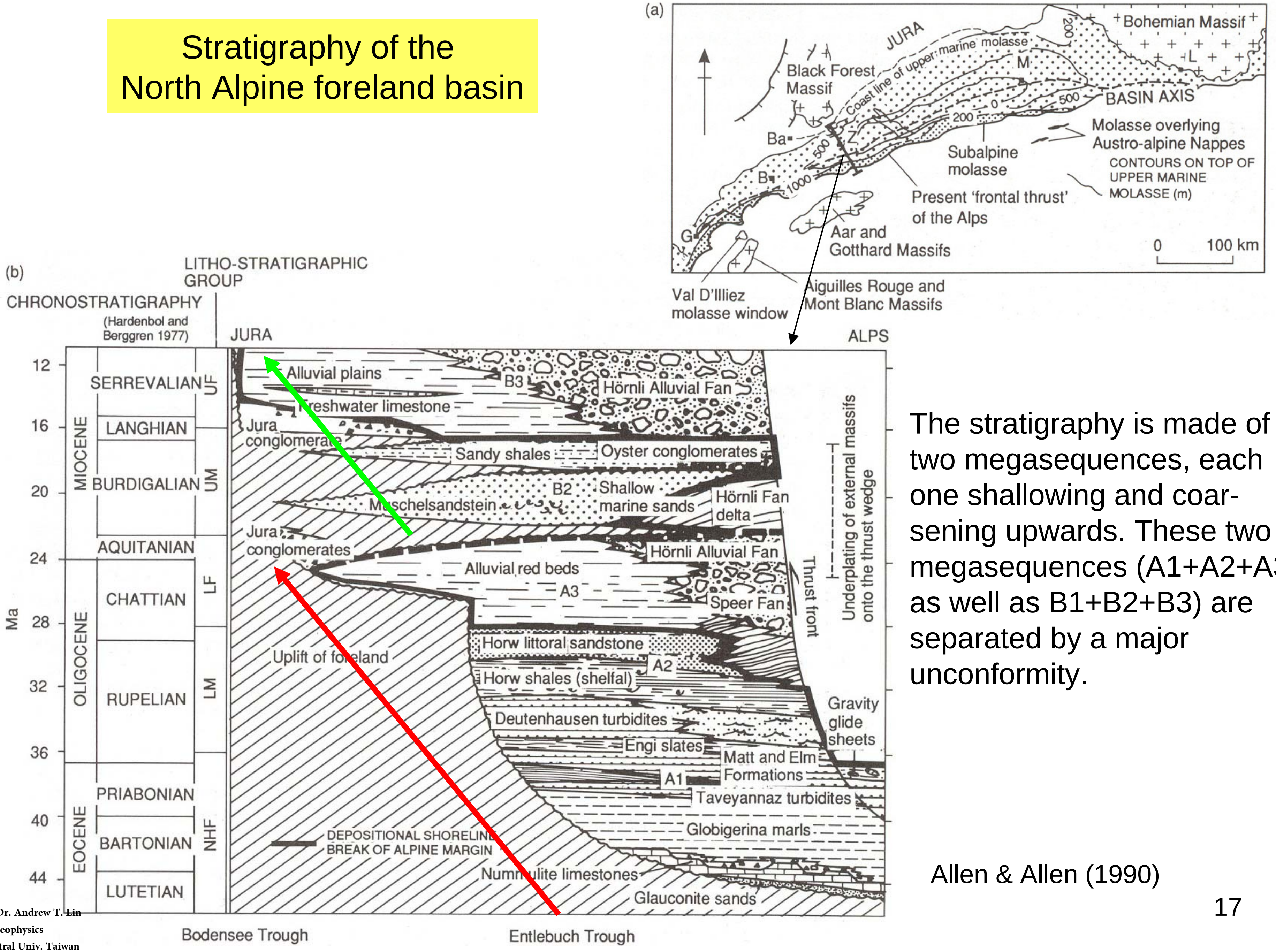

The stratigraphy is made of two megasequences, each one shallowing and coarsening upwards. These two megasequences (A1+A2+A3 as well as B1+B2+B3) are separated by a major unconformity.

Allen & Allen (1990)

Prepared by Dr. Andrew T. Lin
Institute of Geophysics
National Central Univ. Taiwan

Episodic thrusting and unconformity development (a, b)
vs.
constant thrusting but varying eustasy (c, d)

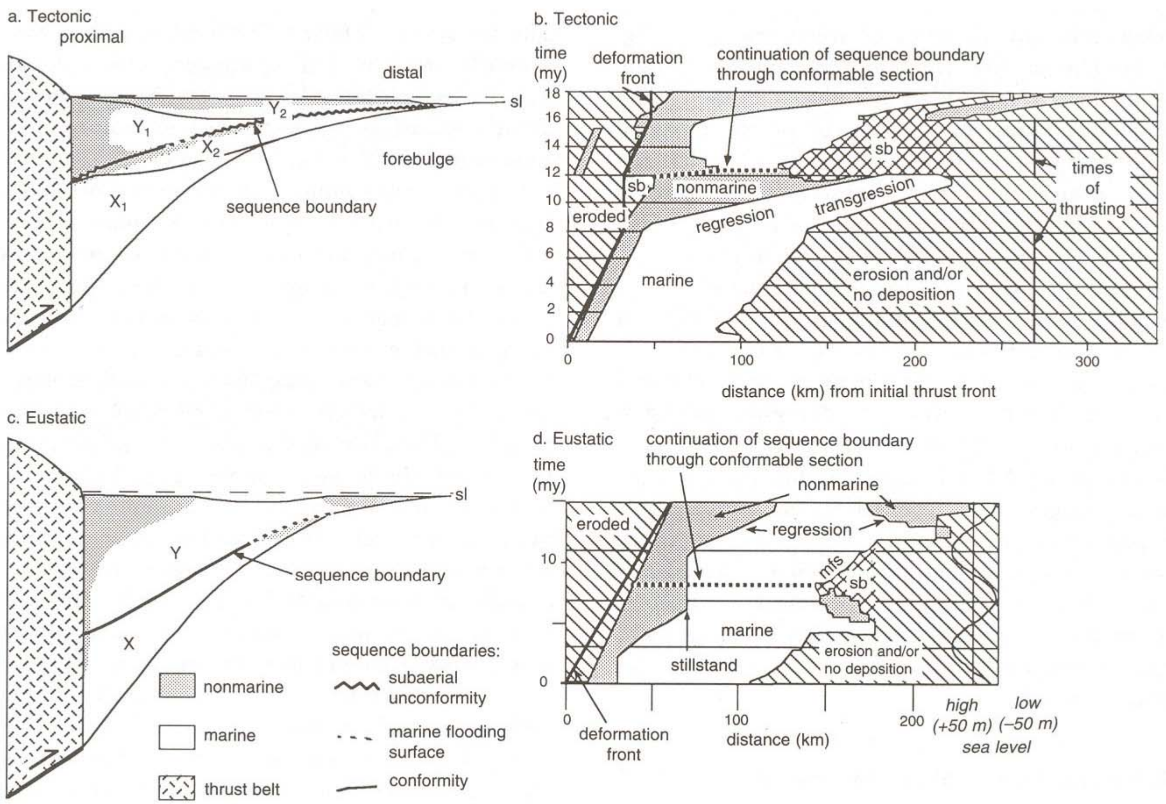

Fig. 9.11 Comparison of marine foreland-basin stratigraphic sequences predicted in response to (A, B) episodic thrusting but constant sea level, and (C, D) eustatic sea-level change but steady thrusting. Two models use identical parameters, except for thrust timing and eustatic variation. Eustatic variation generates an unconformable sequence boundary on the distal basin margin, which is traced into the proximal zone along conformable surfaces, and separates sequences X and Y. Eustatic variation causes stillstands and regressions (and with other values of the parameters, transgressions) but little erosion or progradation on the proximal margin. mfs = marine flooding surface; sb = sequence boundary (time and area that are incorporated in sequence-bounding unconformity shown by crossing-diagonal pattern). Episodic tectonism generates an unconformable sequence boundary across much of the basin (see text). X1 and Y1 are the syndeformational hemicycles, during whose deposition the basin is narrow and facies first retrograde and then stack vertically; X2 and Y2 are the quiescent hemicycles, during whose deposition considerable progradation occurs. A greater width is shown in B than in A because, although distal strata are widespread, they are too thin to resolve at scale of A. In cross sections, left margin of basin (located at position of deformation front at end of time interval) is shown as vertical line, to avoid the visual complications of deformed sequences. Two cycles are shown for each case, comprising 18 million years in A, B, and 16 million years in C, D. After Jordan and Flemings (1991).

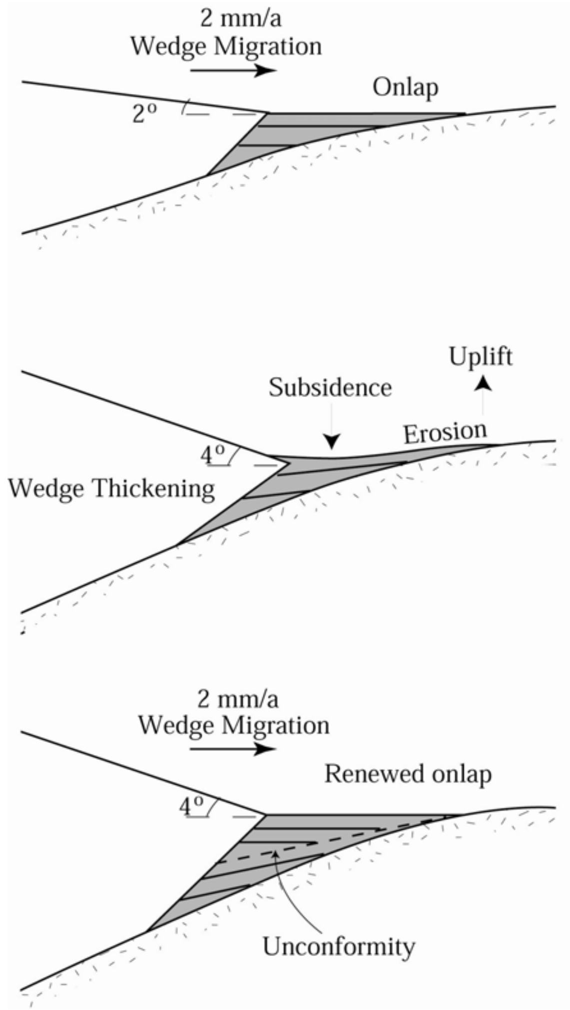

Sinclair et al.'s (1991) model for the origin of the basin-wide unconformities in foreland basins by thrust-and-fold load migration and wedge thickening on an elastic plate.

Prepared by Dr. Andrew T. Lin
Institute of Geophysics
National Central Univ. Taiwan

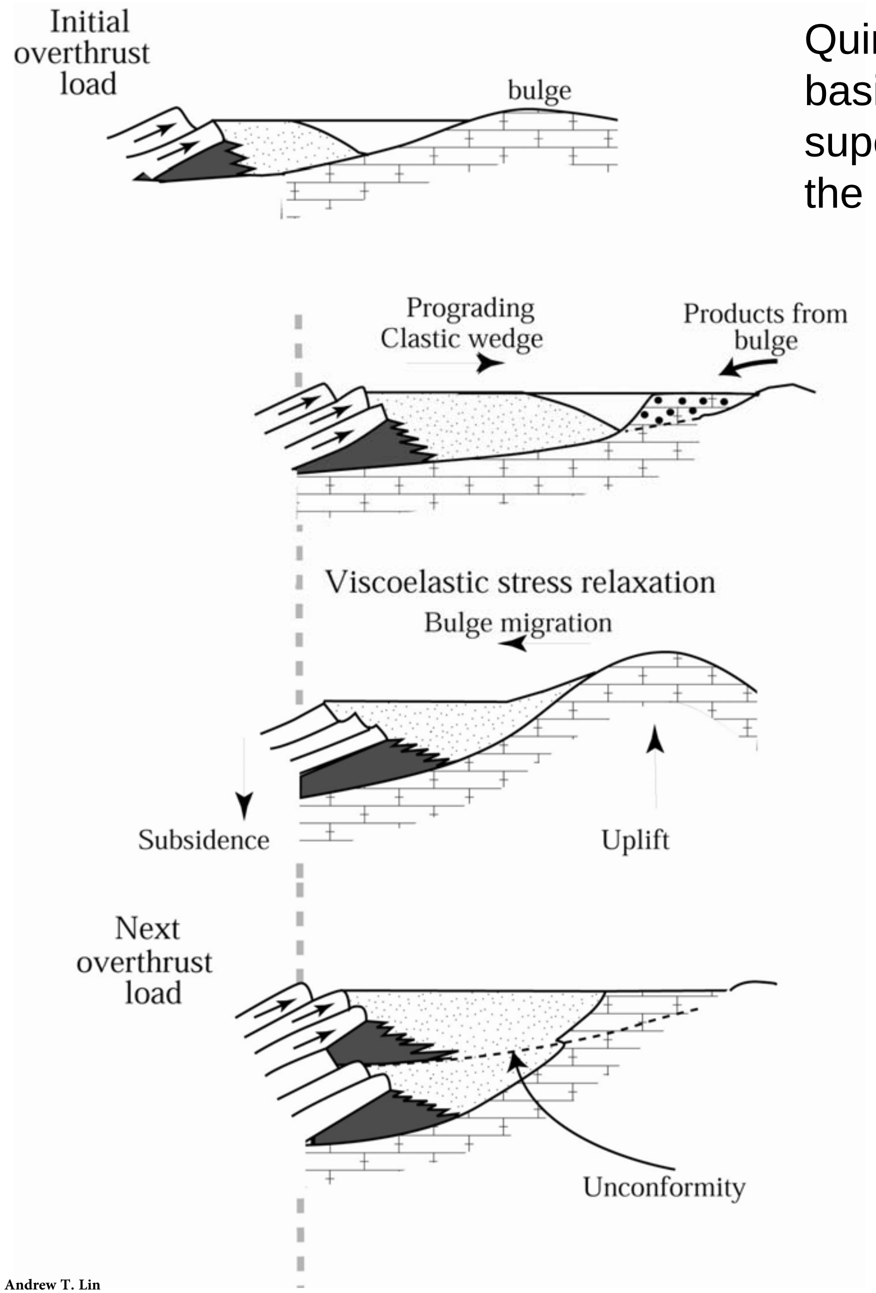

Quinlan & Beaumont’s (1984) model for the origin of basin-wide unconformities in foreland basins by the superposition of successive thrust-and-fold loads on the surface of a viscoelastic plate.

Viscoelastic model
T_e = 67 km, τ =27.5 Myr.

Subsidence curves for the Rocky Mountain foreland basins

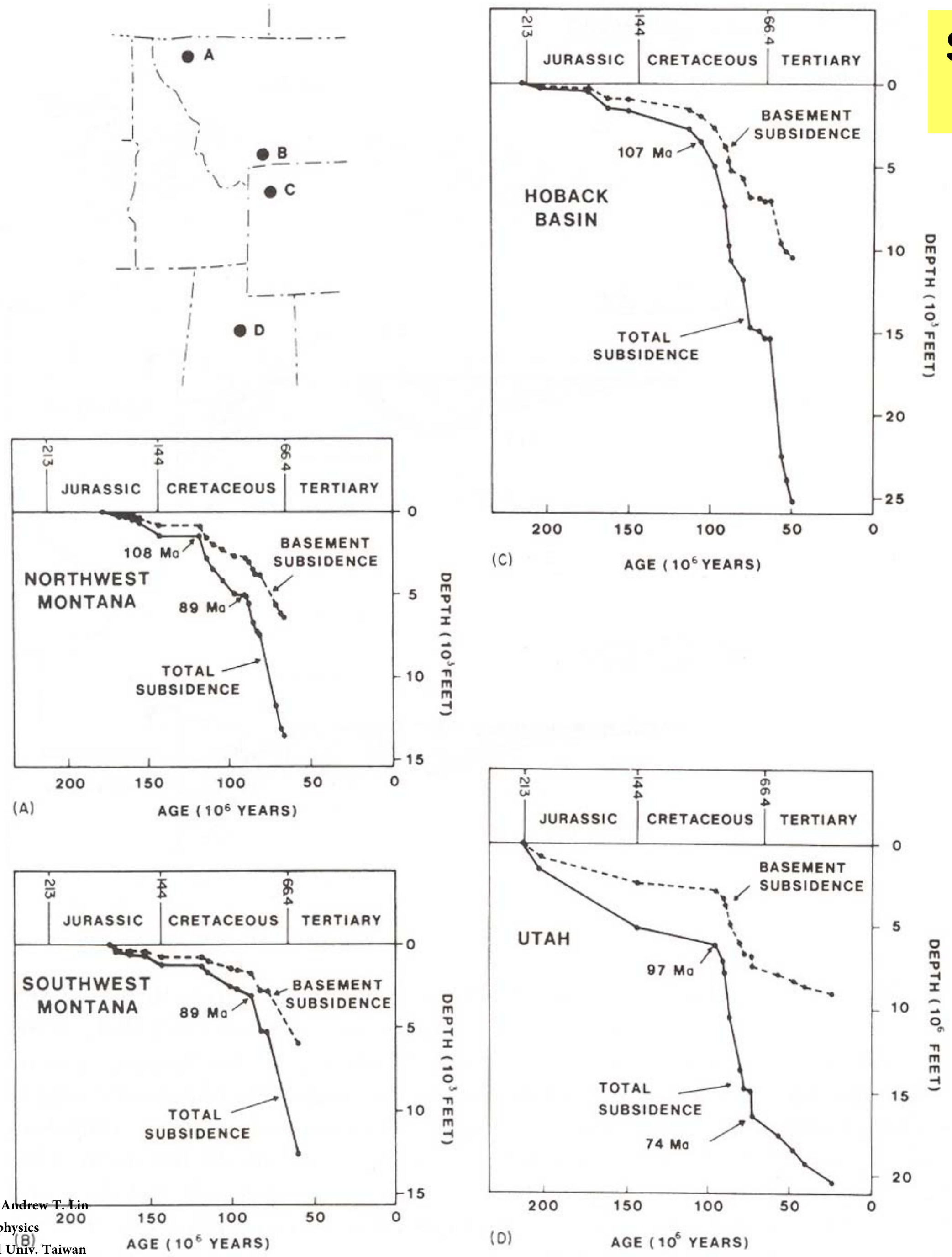

The characteristic convex-up shape, with inflexion points corresponding to thrust-loading events.

Cross (1986)

Prepared by Dr. Andrew T. Lin
Institute of Geophysics
National Central Univ. Taiwan

Filling up of foreland basins

Underfill

Overfill

Crampton & Allen (1995)

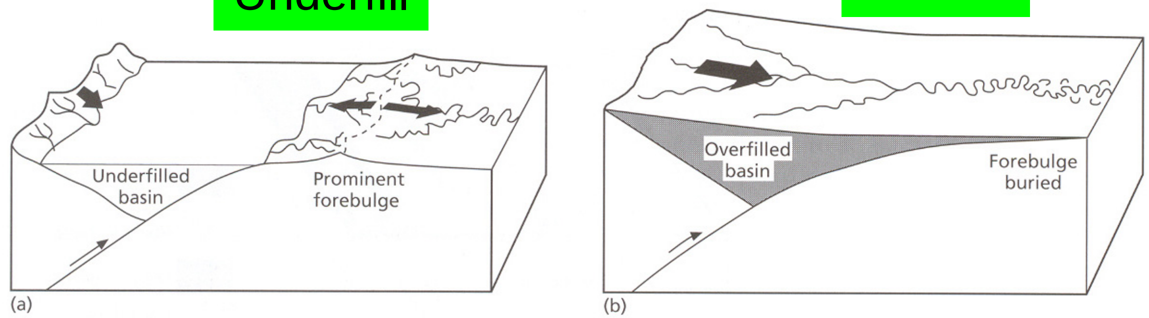

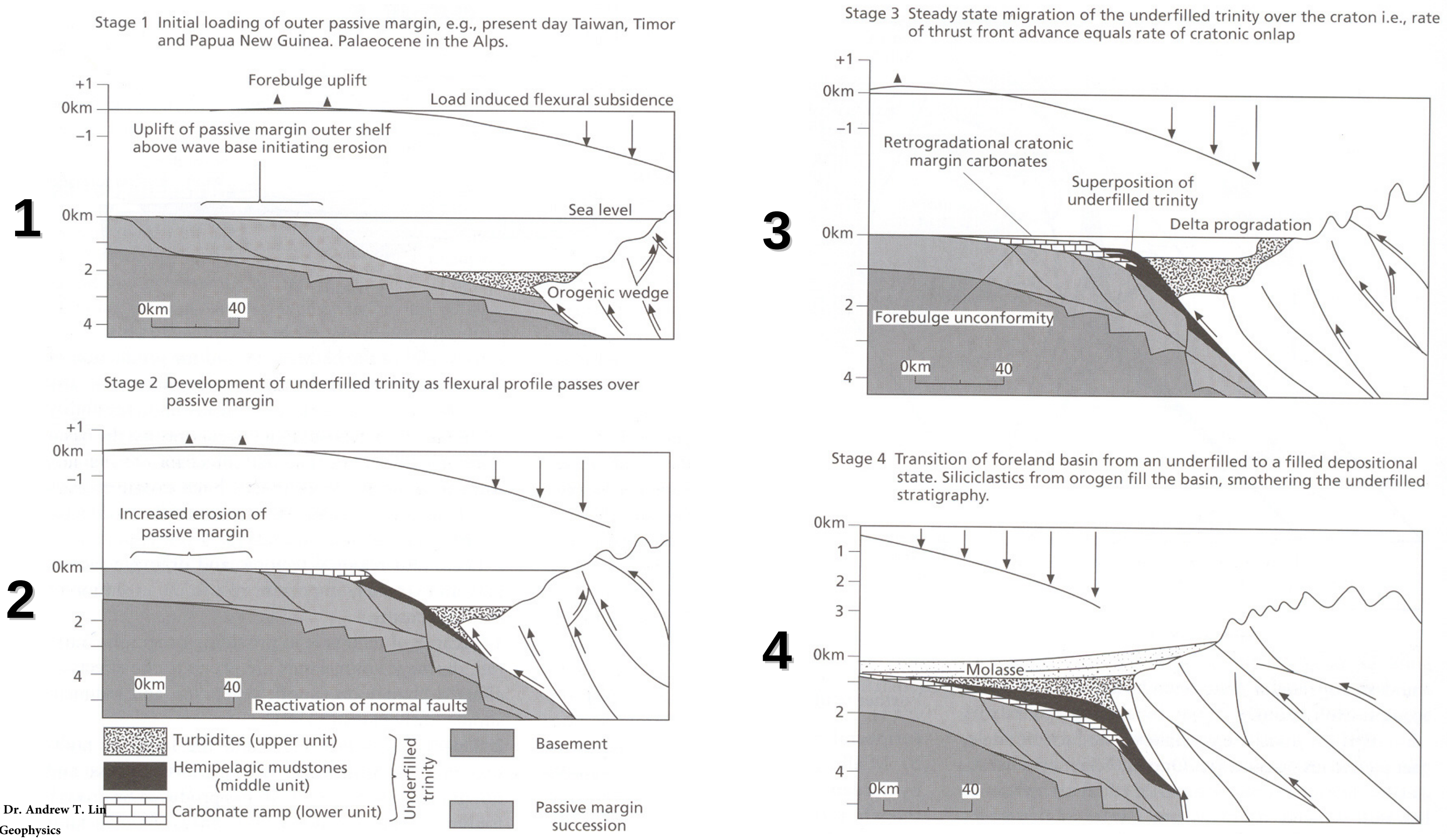

Sinclair (1997)

Lithospheric strength and structural styles (thin- or thick-skinned deformation) in the fold-and-thrust belt

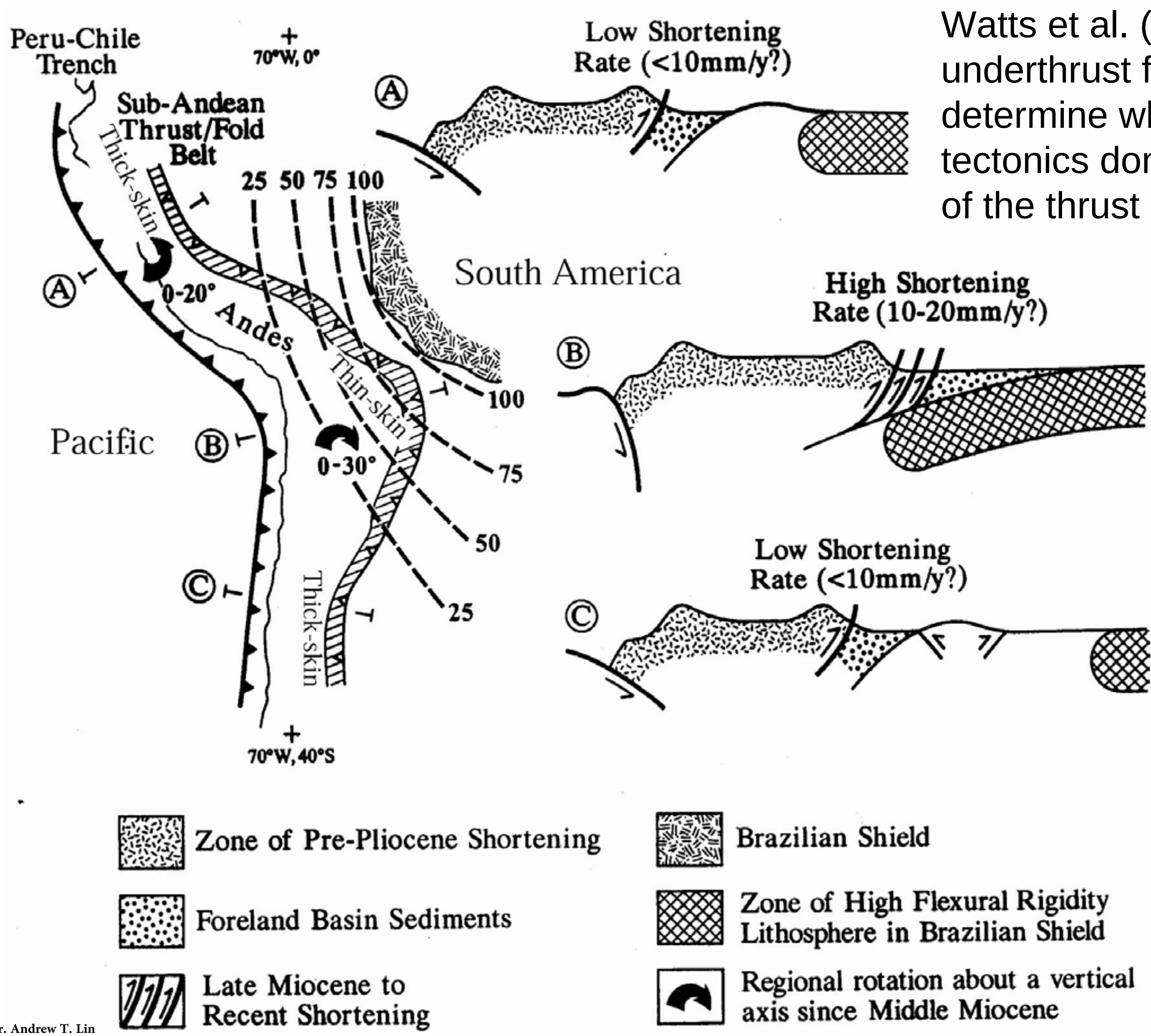

Watts et al. (1995) suggest that T_e of the underthrust foreland lithosphere may determine whether thin-skin or thick-skin tectonics dominate the style of deformation of the thrust and fold belt.

High T_e ⟶ Thin-skin

Low T_e ⟶ Thick-skin (basement involved)

Note:
Others indicated that it is the dips of the subducting plate that determine the thin- or thick-skin tectonics.

High angle ⟶ Thin-skin

Low angle ⟶ Thick-skin

Prepared by Dr. Andrew T. Lin
Institute of Geophysics
National Central Univ. Taiwan